This document contains the draft version of the following paper:

A. Ananthanarayanan, C. Thamire, and S.K. Gupta. Investigation of revolute joint clearances created by in-mold assembly process. *IEEE International Symposium on Assembly and Manufacturing*, Ann Arbor, Michigan, July 2007.

Readers are encouraged to get the official version from the conference proceedings or by contacting Dr. S.K. Gupta (skgupta@umd.edu).

Investigation of Revolute Joint Clearances Created by an In-Mold Assembly Process

Arvind Ananthanarayanan, Chandrasekhar Thamire, and Satyandra K. Gupta

***Abstract*— Revolute joints are frequently used in articulated structures. Traditionally, such a joint is formed by assembling two components. As an alternative, revolute joints can be created inside the mold using an in-mold assembly process. This process eliminates the need for post-molding assembly, thus significantly reducing the cycle time and part count. The functional performance of a revolute joint depends on the clearance in the joint. The clearance in turn depends on the part shrinkage and the mold deformation during the molding process. The presence of a polymer part during the second molding stage makes an in-mold assembly process significantly different from the traditional molding process due to the difference in heat transfer and deformation characteristics. This paper presents experimental data and a preliminary model to explain the differences in clearance produced by an Aluminum mold and an Aluminum mold with an Acrylonitrile butadiene styrene (ABS) insert. Our data indicates that there is a significant difference between the clearances observed from these two different types of molds. We believe that clearances produced depend strongly on the thermal history of the parts.**

I. INTRODUCTION

INJECTION molding is a popular manufacturing process for mass producing plastic parts. Using this method, parts of reasonable mechanical strength, surface finish, and complex geometry can be easily produced. Moreover, parts produced do not normally require secondary processing. When relative motion between such parts warrants assembly, they are manually assembled to create articulated joints. The assembly process, however, can be time consuming and labor intensive.

In-mold assembly process presents an alternative way of creating articulated joints. In this process, molding operations are performed in multiple molding stages and assembled parts are directly produced inside the mold, eliminating the need for post-molding assembly operations. The expected benefits include reduced cycle time and part count, the latter due to elimination of fasteners.

Figure 1 shows a revolute joint that can be produced using an in-mold assembly process. The steps involved in molding this joint are the following:

1) The frame is first molded in the first stage mold using a high melting-point polymer.
2) The frame is inserted into the second stage mold next.
3) The second stage part is then molded in the cavity formed from the first stage part and the second stage mold, using a lower melting-point polymer.
4) Upon cooling, the in-mold assembled part with a revolute joint is ejected from the mold.

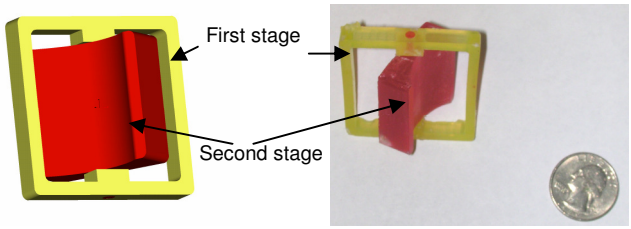

Fig. 1. A revolute joint produced using an in-mold assembly process

Polymers used in the second stage are typically of a lower melting point compared to those used in the first stage. This is to ensure that the first stage polymer does not melt during the injection of the second stage part, which will promote an adhesion-free revolute joint. Since the performance of the joint relies heavily on the clearance between the constituent parts, it is important to achieve the design clearances.

Figure 2 presents a simplified illustration of joint clearances formed in In-Mold Assembly processes. The first stage part acts as a mold insert during the molding of the second stage part and undergoes deformation due to the process pressure and temperature in the second stage. This changes the effective size of the cavity from d to d_m. During solidification, shrinkage occurs in the second stage part causing its final dimension d_p to be different from d or d_m. Further, as the injection pressure is removed and cooling occurs, the first stage part may recover some of the

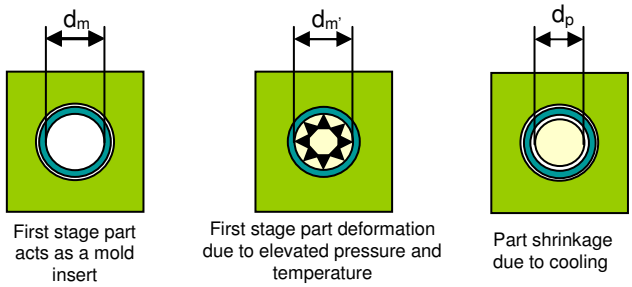

Fig. 2 Clearances in in-mold assembled joints

mechanical deformation and expansion it has undergone

Manuscript received December 16, 2006.

Arvind Ananthanarayanan is with the Mechanical Engineering Department University of Maryland, College Park, MD 20742 USA (e-mail: arvinda@umd.edu).

Chandrasekhar Thamire, is with the the Mechanical Engineering Department, University of Maryland, College Park, MD 20742 USA (e-mail: cthamire@umd.edu).

Satyandra K Gupta is with the Mechanical Engineering Department, University of Maryland, College Park, MD 20742 USA (Corresponding author phone: 301-405-5306; e-mail: skgupta@umd.edu).

earlier. The final clearance between the two parts is then determined by the deformation retained by the first-stage part and the shrinkage produced in the second-stage part.

The presence of a polymer during the second molding stage makes an in-mold assembly process significantly different from a single-stage molding process. For tool steel or aluminum molds, mold deformation can be considered to be negligible, compared to the shrinkage values. On the other hand, in In-Mold Assemblies, the first stage part has a stiffness lower than tool steel and aluminum and hence may undergo considerable deformation, which should be considered in assessing clearances. Further, thermal behavior of polymers is different from those of metals and alloys, which can affect cooling of the second-stage parts significantly. This in turn may affect the shrinkage and hence needs to be considered for estimating the clearances.

In this study, clearances formed during the in-mold assembly of an injection-molded revolute joint comprising a cylindrical sleeve and pin are examined, with the sleeve molded in the first stage and the pin in the second. To better understand the process, pins of similar size were also molded in Aluminum molds directly, without the polymer sleeves. Experimental data is presented for three joint sizes. A preliminary theoretical model is proposed to understand the differences observed in clearances with an Aluminum mold and Aluminum mold with the polymer sleeve.

II. Related Work

Using in-mold assembly for articulated devices is a relatively new technology and there are few studies that outline a systematic methodology for designing parts and molds. Priyadarshi et al. [1] have presented a model for designing In-Mold Assemblies and molding process that enables one to design the joint clearance and variation in the joint clearance to meet the functional goals. They outlined a systematic approach to aid product designers determine part dimensions and material properties, providing proven mold design templates for realizing revolute, prismatic, and spherical joints. Banerjee et al. [2] have recently presented a comprehensive review of multi-material injection molding (MMM) processes. They presented an approach for systematically identifying potential manufacturability issues that are unique to such processes and proposed design rules to avoid such problems. Their analysis shows that the rules applicable for traditional single material molding need to be suppressed or modified sometimes for the MMM processes.

Several studies have examined modeling of in-mold shrinkage of thermoplastics in metallic molds. A simple model describing the shrinkage by following the Pressure-Volume-Temperature (PVT) diagram from glass transition to ambient conditions and obtaining the final product volume was considered in early studies [3]. Jansen and Titomanlio [4, 5] examined the effects of pressure and Poisson expansion on thickness shrinkage through a thermoelastic model. Effect of processing conditions on shrinkage of four amorphous resins and two semicrystalline materials was investigated in a study by Jansen et al. [1]. A thermoelastic model was presented that described the shrinkage of amorphous materials well, but overpredicted that of crystalline materials. A model describing the anisotropic shrinkage of amorphous [7] and semicrystalline [8] polymers was proposed by Kwon et al. [7, 8], based on the frozen-in orientation function and elastic recovery determined from a non-linear viscoelastic constitutive equation. Their predicted results were in fair agreement with the experimental results. Delaunay et al [9] examined the possibility of mold deflection due to injection and packing pressure changing the basic shape of the cavity and hence affecting the overall shrinkage. Bushko and Stokes [10, 11] modeled the mechanics of part shrinkage and warpage and residual stresses and strains for the solidification of a molten layer of amorphous thermoplastic material between cooled plates, assuming thermo-viscoelastic behavior for the material. Similarly, a number of other studies involving shrinkage-prediction models based on process parameters and material variables have been reported. The reader is referred to [3-11] for an elaborate review of such studies. While several important results were produced from these investigations, most of the published studies were focused on shrinkage of polymers in tool steel and Aluminum or other hard metallic molds. No work appears to have been reported addressing the shrinkage of polymers in soft molds. The current study attempts to initiate such a study, in the context of in-mold assembly processes for manufacturing rigid-body joints.

III. Experimental Setup

As described earlier, an in-mold assembly typically involves the part molded in the first stage as a mold insert for the second stage (Fig. 1). To examine clearances obtained in an In-Mold Assembled joint, we have utilized components featuring cylindrical geometry because of axisymmetry considerations. Thus to manufacture an In-Mold Assembled revolute joint, a cylindrical sleeve was first molded in the first stage. This part was subsequently used as a mold insert for the pin in the second stage. Upon cooling, an In-Mold Assembled revolute joint was produced. The methodology of molding the pin into the hole employed in the study enabled us to examine situations where running clearances were desired.

The parts tested were made from low-density Polyethylene (LDPE). In order to compare the shrinkage between hard and soft molds, parts of different sizes were molded in aluminum as well as sleeves made from Acrylonitrile butadiene styrene (ABS). The parts were injection molded in Milacron's Babyplast Injection molding machine. The mold assembly consisted of an ABS sleeve and an LDPE pin within an Aluminum housing for the in-mold assemblies and an LDPE pin in an Aluminum mold for the single-stage molding. For the latter case, Aluminum molds were machined and the LDPE parts were molded using molds thus created.

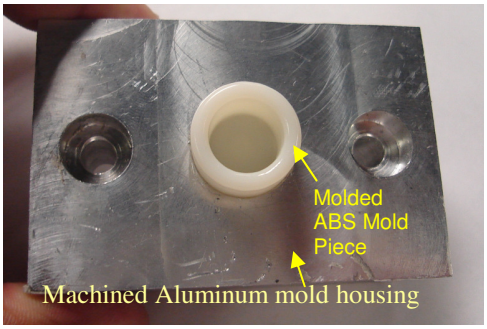

Fig. 3. Mold assembly shown with the ABS sleeve

The process for obtaining the ABS sleeves involved the following steps: Molds for making the ABS mold inserts were first machined. ABS sleeves were then made using these molds. Aluminum mold housings were machined next. Finally mold assemblies consisting of ABS molds and the Aluminum housings were assembled (Fig. 3). LDPE parts were next molded using these mold assemblies.

Three sizes of pins were used in the experiments, with nominal diameters of ¼", 3/8", and ½". Since clearances obtained using different mold materials were of primary interest, most of the other variables were held constant through scaling. Lengths were kept the same as diameters to retain an aspect ratio of unity for the parts. Injection pressure and temperature were kept constant at 700 bars and 130°C. Part diameter was used as the scaling length and the diameter to injection-time ratio as the scaling velocity. Cooling times were scaled by the ratio of the square of the diameter to the thermal diffusivity of the part material. This resulted in constant scaled pressures and cooling times for all sizes used. Scaled thickness for ABS inserts, however, could not be maintained constant due to machining constraints.

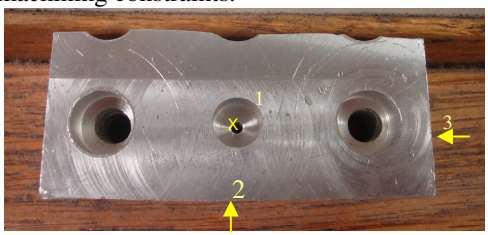

Fig. 4 Positions of thermocouples for Al mold

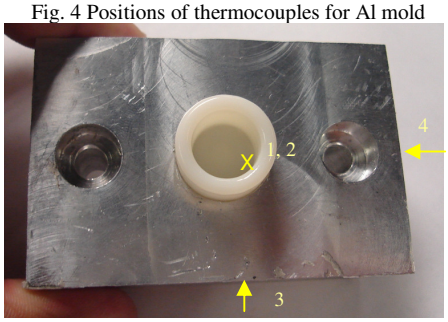

Fig. 5 Positions of thermocouples for ABS mold

Five LDPE parts were molded for each size with and without the ABS inserts. DOW Polyethylene 722 was used as the part material, Hival ABS HG6 Natural® was used for ABS inserts, and an Aluminum-based alloy was used for Aluminum mold pieces.

Dimensions of ABS inserts and Aluminum molds were measured before and after molding. The LDPE parts were measured after molding and subsequent cooling to constant scaled cooling times. Temperatures at locations indicated in Fig. 4 and Fig. 5 were measured for three sets of 3/8" and ½" parts, using a National Instruments data acquisition system that included a PCI-4221 data acquisition card, SCXI 1000 and 1102 modules, and a TC-2095 thermocouple panel. Four K-type thermocouples were used to measure temperatures for configurations involving ABS, while three were used for those not involving ABS. Two were attached to the mold surfaces, one at a point centrally located within the mold for measuring the temperature history of the parts, and a fourth one, if applicable, at the base of the ABS insert for evaluation of heat transfer through the insert. The thermocouple at the central point in the mold was held in position using a rigid copper tube through which the thermocouple was passed.

IV. THEORY

Assembly clearance in in-mold assemblies is affected by a variety of parameters, including the clearance between the mold and the insert, physical properties of the materials, temperature and pressure histories, geometry, and process parameters. In the model proposed here, we assume that such an assembly clearance occurs due to the deformation of the polymer insert at the elevated pressure and temperature it is subjected to, thermal expansion of the polymer insert, volumetric shrinkage due to enhanced crystallization from reduced heat transfer, and volumetric expansion due to solidification under pressure. For simplicity, creep and relaxation effects are not included. In cylindrical geometry, the diametrical clearance at any time t after the solidification has ended may then be expressed as

$$C(\theta,z,t) = \delta_I(\theta,z,t) + \int_{-R}^{R}\{\alpha(T_s - T(\theta,z,t)) + \delta_{cr} - \beta(P_s - P(t))\}dr. \quad (1)$$

In the above expression, C is the diametrical clearance, T is the instantaneous temperature at the location of interest, P_s is the pressure during solidification, P is the instantaneous pressure in the polymer part, and δ_I is the permanent deformation retained by the ABS insert. The remaining parameters pertain to LDPE: α is the linear thermal expansion coefficient, T_s is the solidification temperature, δ_{cr} is the crystallinity factor, and β is the compressibility. R is the radius of the pin and θ and z are the angular and axial coordinates, respectively. The expression provided above is similar to that developed by Jansen and Titomanlio [4], and Titomanlio and Jansen [5], and Jansen et al. [1], but differs from theirs due to the terms representing the deformation of the insert and temperature-dependent crystallinity during curing.

To evaluate δ_I and P, one needs to examine the flow characteristics of the melt, while heat transfer should be examined for calculating δ_{cr} and T. In the current study, these were performed in the following manner. First the non-isothermal flow problem was solved to evaluate the pressures

occurring during solidification and at the insert. Heat transfer was then evaluated to determine the thermal expansion component and shrinkage due to crystallization. For the flow problem, the governing equations are given by

$$\frac{\partial \rho}{\partial t} + \nabla.(\rho \underline{V}) = 0 \tag{2}$$

$$\frac{\partial(\rho \underline{V})}{\partial t} + \underline{V}.\nabla(\rho \underline{V}) = \nabla.\left\{-P\underline{I} + \mu\left(\nabla \underline{V} + \nabla \underline{V}^{T}\right)\right\} + \rho \underline{b} \tag{3}$$

$$\rho c_p \left(\frac{\partial T}{\partial t} + \underline{V}.\nabla T\right) = k\nabla^2 T + \mu\dot{\gamma}^2 + \dot{\zeta}\Delta H \tag{4}$$

Where $\dot{\gamma}$ is the rate of shearing strain, $\dot{\zeta}$ is the rate of solidification, c_p is the specific heat capacity, k is the thermal conductivity, ΔH is the exothermic heat of polymerization, μ is the dynamic viscosity, ρ is the density, and $\underline{V}$ is the velocity vector, $\underline{b}$ is the body-force vector. $\dot{\zeta}$ was evaluated using a model proposed by Kamal and Ryan [12] because of its ability to match closely with the experimental data. Values for ρ, k, and c_p were taken from references [13-15]. μ was assumed to be of the following form [16]:

$$\mu = m\left(\left|\partial V_z / \partial r\right|\right)^{n-1} \tag{5}$$

"m" in the above equation represents the Newtonian viscosity, whereas *"n"* represents the deviation from the Newtonian fluids, which is smaller than unity for most polymer melts [14].

The governing equations were solved under the assumption of axisymmetry. Body forces were neglected and a fully-developed flow was assumed at the flow front. Boundary conditions assumed were no-slip condition at the interface between the insert and the part, axisymmetry along the axis, pressure being atmospheric at the flow front [15], and a constant flowrate condition at z = 0, determined from experimental conditions. Convection boundary conditions were assumed for the temperature field outside of the Aluminum mold and at the mold front, while the processing temperature was assumed to be held until the gate shut-off occurs at z = 0.

Because of the energy dissipation term in the energy equation, the velocity profile and pressures were initially guessed and the temperature field was calculated. A new viscosity profile was then calculated using the new temperature profile. The linear momentum equation was solved next to calculate the new velocity profiles. Newton-Raphson method [17] was applied for convergence of pressures and the velocity profiles for the calculated temperature values. With the new values for the velocity field, the temperature field was calculated again, and the procedure was repeated until convergence criteria were met for both the temperature and velocity fields. The solution was then marched in the z direction in the manner described above, till the end of the cavity was reached. Filling times and pressure distributions were noted for use in the clearance computations at a later stage.

To obtain the thermal history, energy equation was solved next. The cooling polymer, surrounding ABS sleeve, when applicable, and the Al mold were considered. In cylindrical coordinates, the governing equation for this step may be written as:

$$\left(\frac{\partial(\rho c_p T)}{\partial t}\right) = \frac{1}{r}\frac{\partial}{\partial r}\left(k_r r \frac{dT}{dr}\right) + \frac{1}{r^2}\frac{\partial}{\partial \theta}\left(k_\theta \frac{\partial T}{\partial \theta}\right) + \frac{\partial}{\partial z}\left(k_z \frac{\partial T}{\partial z}\right) + \rho \zeta_\infty \Delta H_c \frac{d\xi}{dt} \tag{6}$$

In the above equation, ζ_∞ is the maximum possible crystallinity for the material, ΔH_c is the exothermic heat of crystallization per unit mass, and ξ is the relative crystallinity. The governing equations for the ABS sleeve and Aluminum mold are similar to (6), with the exception that the heat generation term due to change in crystallinity is assumed to be absent. Boundary conditions applied were natural-convection boundary conditions on all sides of the mold except at the nozzle location, a perfect thermal contact at the interfaces during the application of the holding pressure, and axisymmetry at the axis. Thermal contact conductance was replaced by a convection condition with convection coefficients applicable for natural convection in cylindrical annuli. This was included to account for the gap conductance that arises once shrinkage begins. After the ejection time, natural-convection boundary condition was applied over the surface of the part and the inner diameter of the ABS insert. θ–dependence was kept in the equation to examine the effect of non-uniform thermal contact at the contact region for use in later studies.

The governing equation was integrated numerically using the Alternating Direct Implicit (ADI) method [18] subject to the boundary and initial conditions. Initially, zero crystallization was assumed and the temperatures were calculated based on an initial estimate of the properties. After each time step, properties were adjusted to match the temperature distribution calculated. This process continued until steady state was reached. Steady state solutions were considered converged when the maximum change in the local values of T and in each of the global energy rates at the exterior surfaces became less than 10^{-4} percent. Grid size was refined when any of the above requirements was not satisfied. Grid-independence was checked for all three sizes used in the experiment. Spatial resolution was varied from 21 to 101 in the z direction, from 21 to 81 in the r direction, and from 17 to 97 in the θ direction. Grid independence was noted for grids finer than 51 x 41 x 41. For the calculations considered here, a grid size of 61x61x49 was used.

Temperature histories calculated at the center of the injected part were compared with those measured. Curing kinetics were then adjusted in an attempt to match the temperature profiles through an iterative process. Once the process was stabilized, property values were adjusted to account for the change in crystallinity in (6), and the crystallinity values and property values were both readjusted iteratively until the calculated values matched the measured values to within 0.1% of the measured values.

Lastly, pressure histories calculated in the flow calculations and holding pressure applied were used to compute the elastoplastic deformation encountered by the surrounding material. A hollow axisymmetric cylinder in plane strain was assumed, with the ends assumed to be restrained. A Mohr-Coulomb failure criterion was assumed to be valid. In the elastic zone, the strain-displacement and linear-momentum equations are given by:

$$\begin{bmatrix} \varepsilon_r \\ \varepsilon_\theta \end{bmatrix} = \begin{bmatrix} \frac{du_r}{dr} \\ \frac{u_r}{r} \end{bmatrix} \tag{7}$$

and

$$\frac{d\sigma_r}{dr} + \frac{\sigma_r - \sigma_\theta}{r} = 0 \tag{8}$$

To determine the extent of the plastic zone that may occur as a result of yielding, the Mohr-Coulomb failure criterion for the maximum principal stress is initially substituted into the linear-momentum balance equation, and integrated. The boundary condition of averaged internal pressure at the inner radius was applied to determine the radial stress distribution in plastic zone. Using the Mohr-Coulomb criterion again, the circumferential stress distribution in the plastic zone was next determined. To determine the boundary between the elastic and plastic zones, the elastic stresses were equated to the stresses in the plastic zone and solved for the radius on the boundary. Using the strain-displacement relationships, radial displacements at the inner surface were finally obtained. All the individual components involved in the calculation of clearance were then added using (1) and compared with the measured values.

V. RESULTS AND DISCUSSION

Average relative clearances measured and calculated are shown in Table 1. Relative clearance considered here is the physical clearance scaled by the measured value of the pin diameter, expressed as a percentage. Relative clearances were analyzed using a 2-way ANOVA procedure [19]. Results indicate that the relative clearances measured differ significantly between the two cases ($p < 0.05$). Multiple comparisons using a Tukey-Kramer procedure [19] show no significant difference between sizes within each material, which may be attributed to the scaling incorporated into the experimental design. Comparison of means between the two molds for individual sizes indicate a significant difference in measured relative clearances for all three sizes.

Sample temperature histories measured along the axis for two pins of size 0.375" are shown in Fig. 6 and Fig. 7. Heat dissipation occurs relatively quickly for the LDPE specimen made directly in the Aluminum mold (fig. 6). Heat transfer calculations performed for pins made in Aluminum molds predict the temperature history well, without requiring many iterations to account for changes in crystallinity. In contrast, Fig. 7 shows a much slower cooling rate for a LDPE pin covered by an ABS insert. Heat rejection rates here are lower than the former case due to the inferior thermal properties of ABS, which then suggests that densification and a higher shrinkage could occur within the LDPE part. This in turn affects the cooling rates and the thermal properties of LDPE due to differences in crystallinity. Thus, the calculations would not match the measurements, unless changes in thermal properties due to changes in crystallinity were included.

TABLE 1 AVERAGE ABSOLUTE AND RELATIVE CLEARANCES

Nominal Dia. (in)	Measured Average Absolute Clearance (in)		Average Relative Clearance (%)			
			Measured		Calculated	
	Al Mold	Mold with ABS Insert	Al Mold	Mold with ABS Insert	Al Mold	Mold with ABS Insert
0.25	0.007	0.010	2.47	4.02	-	-
0.375	0.011	0.013	2.83	3.61	3.09	4.17
0.5	0.015	0.017	2.93	3.46	3.44	4.53

Once changes in specific volume were made accounting for the changes in packing and incorporated into equation (1), including the other components contributing to the clearance mentioned there, clearances calculated for the 0.375" and 0.5" sizes were compared to the measured values. Computed values compared favorably with the measured values for the 0.375" size, with measured averages being 2.83% (Al molds) and 3.61% (ABS molds), against the calculated averages of 3.09% and 4.17%, respectively. Clearance values computed for 0.5" size, however, exhibited large deviations from the measured values.

Clearances computed exhibit the same trend as the measured values, predicting higher clearances for assemblies made using ABS inserts. While the model overpredicts the clearances by values up to 31% (about 18% for Al molds), it promises to be a useful tool, once more parametric studies are performed to evaluate the functional form of the final correlation and thus enhance its predictive capability.

Plastic deformation of the ABS inserts does not appear to be a significant factor, accounting to less than 7% of the total clearances observed. Since the model does not assume an interference fit at the outer diameter, this result may not be valid for all the cases and needs to be further examined. For geometries where outer diameter of the inserts is constrained, the resulting interfacial pressure will act as an external pressure on the insert and as an internal pressure on the mold and will have to be considered in the calculations.

From a design perspective, clearances obtained in the experiments in this study appear attractive, as they are in the range of running fits. For example, ANSI B 4.2 [20] provides the limits of a clearance or running fit for a nominal size of 0.375" to be ~{0.003",0.010"}. Comparing this with the mean clearance values of 0.013" measured in 0.375" ABS/LDPE assemblies, it is evident that the in-mold assembly processes appear to be capable of producing good running fits. Though the predictions from the model appear to be comparing favorably with the experimental observations, many

improvements are possible. In the model, flow-induced crystallization, elastic recovery, and more realistic thermal contact conductance values need to be incorporated. Axisymmetry and plane strain assumptions need to be relaxed for more accurate clearance predictions. Thermal contact resistance, which is based on joint clearance, needs to be evaluated more accurately, by measuring temperatures at more locations and accounting for non-uniform contact. This can be an important parameter, as indicated in the study by Sridhar et al. [21]. More experimental results are thus needed to further validate the proposed model.

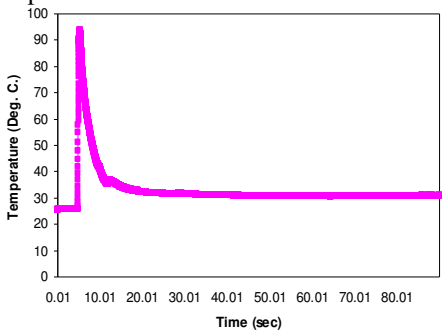

Fig. 6 Temperature History for a 0.375" LDPE specimen molded directly in an Aluminum mold

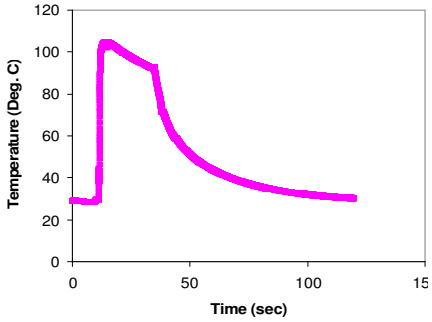

Fig. 7 Temperature History measured for a 0.375" LDPE specimen molded in an ABS insert that was placed in an Aluminum mold**.**

VI. Conclusions

Achieving desired clearances in In-Mold Assemblies made from polymer components is a challenge, from both design and manufacturing perspectives. In the current study, clearances produced for polymer assemblies of three different sizes were examined. Experiments conducted using scaled process parameters revealed statistically significant differences between assembly clearances for polymer parts produced in molds with polymer inserts vs. those produced in purely metallic molds. Hence we will need new models to estimate clearances created by molds with polymer inserts. Possible mechanisms leading to these differences were studied using thermomechanics and finite-difference methods. Though experimental data studied is limited, clearances produced appear to be strongly dependent on the thermal history of the parts. Thus, we believe that thermal properties of materials chosen for the mating parts can strongly influence the assembly clearances produced in polymer assemblies. We are planning to conduct more detailed experimental studies to validate our model.

Acknowledgements

This research has been supported in part by NSF grant DMI0457058 and the Army Research Office through MAV MURI Program (Grant No. ARMY W911NF0410176). Opinions expressed in this paper are those of the authors and do not necessarily reflect opinions of the sponsors.

References

[1] A.K. Priyadarshi, S.K. Gupta, R. Gouker, F. Krebs, M. Shroeder, and S. Warth. Manufacturing multi-material articulated plastic products using in-mold assembly. International Journal of Advanced Manufacturing Technology, 32(3-4):350--365, March, 2007.

[2] A. G. Banerjee, X. Li, G. Fowler, and S. K. Gupta, Incorporating manufacturability considerations during design of injection molded multi-material objects, Res Eng Design, in print.

[3] A. **I.** Isayev and T. Hariharan, Volumetric effects in the injection molding of polymers, Pol. Engg. and Sci., April 1985, Vol. 25, No. 5

[4] K. M. B. Jansen and G. Titomanlio, Effect of Pressure History on Shrinkage and Residual stresses-Injection Molding with constrained Shrinkage, Pol. Engg. and Sci.. Mid-August 1996, Vol. 36, NO. 15

[5] G. Titomanlio and K. M. B. Jansen, In-Mold Shrinkage and Stress Prediction in Injection Molding, Pol. Engg. and Sci.. Mid-August 1996, Vol. 36, NO. 15.

[6] K. M. B. Jansen, D. J. Van Dijk, and M. H. Husselman, Effect of processing conditions on shrinkage in injection molding, Pol. Engg. and Sci., May 1998, Vol. 38, No. 5

[7] Keehae Kwon, A. I. Isayev, K. H. Kim, Toward a Viscoelastic Modeling of Anisotropic Shrinkage in Injection Molding of Amorphous Polymers, Journal of Applied Polymer Science, Vol. 98, 2300–2313, 2005

[8] Keehae Kwon, A. I. Isayev, K. H. Kim, Theoretical and Experimental Studies of Anisotropic Shrinkage in Injection Molding of Semicrystalline Polymers, Pol. Engg. and Sci., 2006, 712-728

[9] D. Delaunay and P. Le Bot, Nature of Contact between Polymer and Mold in Injection Molding. Part II: Influence of Mold Deflection on Pressure History and Shrinkage, Pol. Engg. and Sci., July 2000, Vol. 40, No. 7

[10] W. C. Bushko, V. K. Stokes, Solidification of thermoviscoelastic melts. Part 2: Effects of processing conditions on shrinkage and residual stresses, Polymer Engineering & Science, February 1995, Vol. 35, No. 4.

[11] W. C. Bushko, V. K. Stokes, Solidification of thermoviscoelastic melts. Part 4: Effects of boundary conditions on shrinkage and residual stresses, Polymer Engineering & Science, March 1996, Vol. 36, No. 5.

[12] M. R. Kamal and M. R. Ryan, Injection and Compression Molding Fundamentals, Chap. 4, A. I. Isayev (Ed.), Marcel Dekker Publisheers, New York, 1987.

[13] R. Talreja and J, and A.E. Månson, Eds., Polymer Matrix Composites, Elsevier, First Ed., 2001.

[14] F. P. Incropera and D. P. DeWitt: Fundamentals of Heat and Mass Transfer, Fifth Ed., 2001.

[15] G. W. Ehrenstein, G. Riedel, and P. Trawiel, Thermal Analysis of Plastics, Hanser, 2004.

[16] C. D. Han, Rhoelogy is Polymer Processing, Academic Press, New York, 1976.

[17] Ralston, A. and Rabinowitz, P., A First Course in Numerical Analysis, 2nd ed., McGraw-Hill, New York, 1978.

[18] Roache, P., Computational Fluid Dynamics, Hermosa Publishers, Albuquerque, 1976.

[19] J. Devore and N. Farnum, Applied Statistics for Engineers and Scientists, Duxbury Press, Pacific Grove, CA, 1999.

[20] ANSI B 4.2, Preferred Metric Limits and Fits, American National Standards Institute.

[21] L. Sridhar, B. M. Sedlak, and K. A. Narh, Parametric Study of Heat Transfer in Injection Molding – Effect of Thermal Contact Resistance, Journal of Manufacturing Science and Engineering, Transactions of the ASME, Novermber 2000, Vol. 122, 698-705.